Collaborative Project (large-scale integrating project)
Grant Agreement 226273
Theme 6: Environment (including Climate Change)
Duration: March 1st, 2009 – February 29th, 2012

SEVENTH FRAMEWORK PROGRAMME

WISER

Water bodies in Europe: Integrative Systems to assess Ecological status and Recovery

DELIVERABLE

Deliverable D3.1-3, part 2: WISER temporal uncertainty analysis for phytoplankton

Lead contractor: **(CEH)**
Contributors: **Stephen Thackeray, Michael Dunbar, Claire McDonald & Bernard Dudley**

Due date of deliverable: **Month 33 (November 2011)**
Actual submission date: **Month 36 (February 2012)**

Project co-funded by the European Commission within the Seventh Framework Programme (2007-2013) Dissemination Level		
PU	Public	X
PP	Restricted to other programme participants (including the Commission Services)	
RE	Restricted to a group specified by the consortium (including the Commission Services)	
CO	Confidential, only for members of the consortium (including the Commission Services)	

Content

Content 2
Approach and rationale 3
Chlorophyll *a* (Chl-*a*) concentration 5
PTI metric 11
Total cyanobacterial biovolume (TCB) 16
Key messages 21
References 22

Approach and rationale

The broad objective of this analysis has been to quantify and compare the degree of temporal (inter-annual and monthly) and spatial (among countries and waterbodies) variation in lake phytoplankton metrics. The three focal metrics have been chlorophyll *a* concentration, PTI and total cyanobacterial biovolume. Though some previous studies (e.g. SNIFFER work) have aimed to quantify temporal variation in phytoplankton at the scale of a single lake system, we have attempted the complementary approach of conducting a large-scale (pan-European) analysis that will give a more integrated picture of the degree of temporal uncertainty in phytoplankton metrics.

To this end, we statistically modelled metric data calculated from the background dataset. We used linear mixed effects (LME) models to resolve the different independent spatial/temporal components of metric variation, while taking account of the nested (hierarchic) structure of the data set. In simple terms, we constructed a model that described the typical monthly pattern of variation in each metric and that allowed this monthly pattern to be modified as a function of lake attributes that might be expected to affect the course of phytoplankton seasonal succession, and therefore monthly metric variation. For example:

Log_{10}(Chl-a) ~ *f* [(Month*Latitude) + (Month*Longitude) + (Month*Altitude Type) + (Month*Humic Type) + (Month*Lake Type) + (Month*logTP)]

(where month, altitude type, humic type and lake type are categorical variables)

So, in this case, the interaction terms allow the "typical" monthly pattern in log_{10} chlorophyll *a* concentration to change as a function of latitude, longitude, altitude, humic content, lake type (e.g. high alkalinity-very shallow..) and log_{10} total phosphorus concentration. We feel that this makes more sense biologically than assuming the same monthly pattern in all lakes across the geographical range of the background data set. Within each model we set up a nesting (random effects) structure that describes the hierarchic nature of the data set: data from each sampling date are nested within month, which is nested within year, which is nested within lake, which is nested within country. We then went through a process of selecting the best combination of month-waterbody attribute interactions, so that we could remove waterbody attributes from the model if they were having only minimal effects on monthly variation in metrics.

From these models we can obtain estimates of the variance in metric scores that arises:

- Among countries, σ^2_c
- Among waterbodies (within countries) , σ^2_w
- Among years (within waterbodies, within countries) , σ^2_y
- Among months (within years, within waterbodies, within countries) , σ^2_m

The variance σ^2_m represents monthly variations in a given metric that are not captured by the "typical" pattern described by the fitted explanatory variables (the fixed effects). This variance can be interpreted as monthly metric variability around the pattern that is typical of a

given waterbody type. For example, in a "typical year" in a given lake type, we might expect a systematic increase in a metric throughout the summer. However, intra-annual variations in physico-chemical forcing or biotic interactions will generate fluctuations around this typical pattern in any given year, such that we are uncertain of whether any single sample is indeed characteristic of average conditions for the month within which it is collected.

Within the fitted models, a residual metric variance (σ^2_r) is also estimated. Given the model structure described above, this residual variance will represent a number of other sources of metric variability. Within σ^2_r there will be some metric variability associated with shorter-term (i.e. within-month) temporal variations in the phytoplankton assemblage. This variation would have been estimated from instances in the data set where >1 sample per month has been collected. However, there will also be an (unknown) contribution to σ^2_r from other sources, for instance differences in sampling site location, analyst and analytical procedures among samples. In the present analysis it has not been possible to explicitly determine the relative magnitude of the contributions of these sources of variability. Herein, we use σ^2_r as an estimate of the remaining sources of variability inherent in the metrics, after accounting for spatial variability (among waterbodies and countries) and the longer-term (inter-annual, monthly) aspects of temporal variability.

For each of the three metrics we ran:

1) An analysis of all background metric data for which latitude, longitude, altitude, lake type, humic type and TP data were available (dominated by data from N-GIG and CB-GIG, with minor contributions from Alpine-GIG and EC-GIG).
2) Simplified (separate) analyses for N-GIG, CB-GIG and Med-GIG. In these analyses some of the variables used in the more integrated cross-GIG analysis (1) had to be dropped as they were redundant within a single GIG.

In what follows we present results on the relative magnitude of temporal and spatial (among-waterbody/country) metric variation. We specifically estimate the longer-term aspects of temporal variation; monthly and inter-annual scale temporal variation ($\sigma^2_m + \sigma^2_y$). We also present the residual metric variance (σ^2_r) to indicate the importance of other sources of variation, compared to spatial and temporal variation. It is possible to produce effects plots to show how monthly variations in metrics change with waterbody attributes, but this may be better left to a subsequent temporal uncertainty paper?

We also demonstrate the effect of different sampling frequencies upon the level of monthly and inter-annual scale temporal sampling uncertainty. Using the estimated variance components, we calculated a measure of sampling variance to describe the degree of sampling uncertainty in the mean observed value of each metric for a waterbody, when based upon collecting samples from different numbers of years, and/or months within years (see Ralph Clarke's presentations on WISERBUGS):

Monthly and inter-annual scale temporal sampling variance of water body mean =

$$\frac{\sigma^2_y \times (1 - [N_{year}/max_{year}])}{N_{year}} + \frac{\sigma^2_m \times (1 - [N_{month}/max_{month}])}{(N_{month} \times N_{year})}$$

Where:

σ^2_{y} = year-level variance from mixed effects model

σ^2_{m} = month-level variance from mixed effects model

N_{year} = number of years sampled

N_{month}= number of months sampled per year

Max_{month} = maximum number of months that can be sampled per year [for total cyanobacteria and PTI, max_{month} =3 (July-September); for Chl-*a*, max_{month} =6 (April-September)]

Max_{year}= maximum number of years that can be sampled per reporting/monitoring period [set at 6 years; a WFD river basin monitoring cycle]

Chlorophyll *a* (Chl-*a*) concentration

Data on chlorophyll were very heavily skewed, and so they were $\log_{10}$ transformed before further analysis. Analyses used data from April-September. Analyses were conducted using the *nlme*, *MuMIn* and *effects* packages in R (Fox 2003, R Development Core Team 2009, Pinheiro et al. 2010, Barton 2011), assuming Gaussian errors.

- For the cross-GIG analysis, and considering instances where all lake attribute data were present, 34920 rows of data were available, from 3391 waterbodies in 13 countries. All lake typology classes were represented in the data set. The most optimal fitted model for this data set included interactions among all lake typology/location variables and month i.e. with none of the original explanatory variables removed.
- For the N-GIG analysis, 31750 rows of data were available from 2885 waterbodies in 5 countries. In this subset of the data there were relatively few high altitude data, and so these were combined with medium altitude data. In a few months, there were no data for certain lake types. We therefore split lake type into the constituent mean depth type and alkalinity type, to remove this problem. The most optimal fitted models collectively suggested that the monthly pattern of variation in $\log_{10}$ Chl-*a* concentration (in N-GIG) is affected by latitude, longitude, $\log_{10}$TP concentration, alkalinity type, mean depth type and humic type.
- For the CB-GIG analysis, 3053 rows of data were available from 478 waterbodies in 8 countries. Within the CB-GIG, alkalinity type and altitude type were redundant as the vast majority of lakes were of high alkalinity and at low altitude. These variables were therefore omitted from the analysis. The most optimal fitted models suggested that the monthly pattern of variation in $\log_{10}$ Chl-*a* concentration (in CB-GIG) is affected by latitude, longitude, mean depth type and $\log_{10}$TP concentration.

- For the Med-GIG analysis, 463 rows of data were available from 190 waterbodies in 6 countries. However, this dataset is diminished drastically if only taking cases where all waterbody typology variables are known. Therefore, only interactions among monthly patterns in $\log_{10}$ Chl-*a* and $\log_{10}$TP concentration were modelled. Very few incidences of sub-monthly scale sampling were found in this subset of the background dataset, such that models attempting to distinguish monthly and within-monthly variability in metric scores failed to converge. Therefore, only models comparing inter-annual and spatial (among country and waterbody) components of variation could be run.
- Analysis at the cross-GIG scale, as well as for N-GIG and CB-GIG data, suggested that the variance in $\log_{10}$ Chl-*a* concentration among countries and waterbodies was greater than the temporal variance (Table 1). The residual variance σ^2_r (representing other sources of metric variability) was consistently higher than estimates of variability at the monthly and inter-annual scales. Temporal variance was higher in CB-GIG than in N-GIG. For Med-GIG, inter-annual variance in $\log_{10}$ Chl-*a* concentration was less than among country and waterbody variance. As in the case of N-GIG and CB-GIG, the residual variance σ^2_r was high compared to the temporal variance estimate. Please note that, for Med-GIG, σ^2_r will include monthly variation.
- Using the formula for monthly and inter-annual scale temporal sampling variance (above) we can show the extent to which uncertainty in metric values can be diminished when sampling in different numbers of years and months. This has been done for the cross-GIG, N-GIG and CB-GIG analyses, in which it was possible to distinguish monthly and inter-annual variance components (Figs. 1-3). From these analyses, it can be seen that the sampling variance (and associated uncertainty) reduces markedly when increasing the number of months sampled from 1 per year to 2 per year and when sampling in 2-3 years, instead of 1. Of course, sampling in all 6 months of all 6 years, eliminates month and year-level temporal uncertainty completely. However, the cross-GIG and N-GIG analyses suggest that sampling variance can be reduced dramatically by sampling in 2 months, in each of 3 years. Due to the higher level of temporal variability for chlorophyll *a* in CB-GIG, a greater degree of replication would be needed to achieve this same reduction in sampling variance (perhaps 3-4 months in each of 4 years).

Table 1. Components of variation in $\log_{10}$ Chl-*a*, expressed as variances.

Variance component	**Cross-GIG**	**N-GIG**	**CB-GIG**	**Med-GIG**
Country, σ^2_c	0.094	0.036	0.042	0.050
Waterbody, σ^2_w	0.142	0.134	0.146	0.199
Total spatial ($\sigma^2_c + \sigma^2_w$)*	**0.237**	**0.170**	**0.189**	**0.249**
Year, σ^2_y	0.003	0.003	0.018	0.048
Month, σ^2_m	0.015	0.013	0.021	-
Residual, **(σ^2_r)**	0.032	0.030	0.058	0.068
Total temporal ($\sigma^2_y + \sigma^2_m$)	**0.018**	**0.016**	**0.039**	**0.048**

*spatial variance components were derived from a mixed-effects model with an intercept only (i.e. a null model).

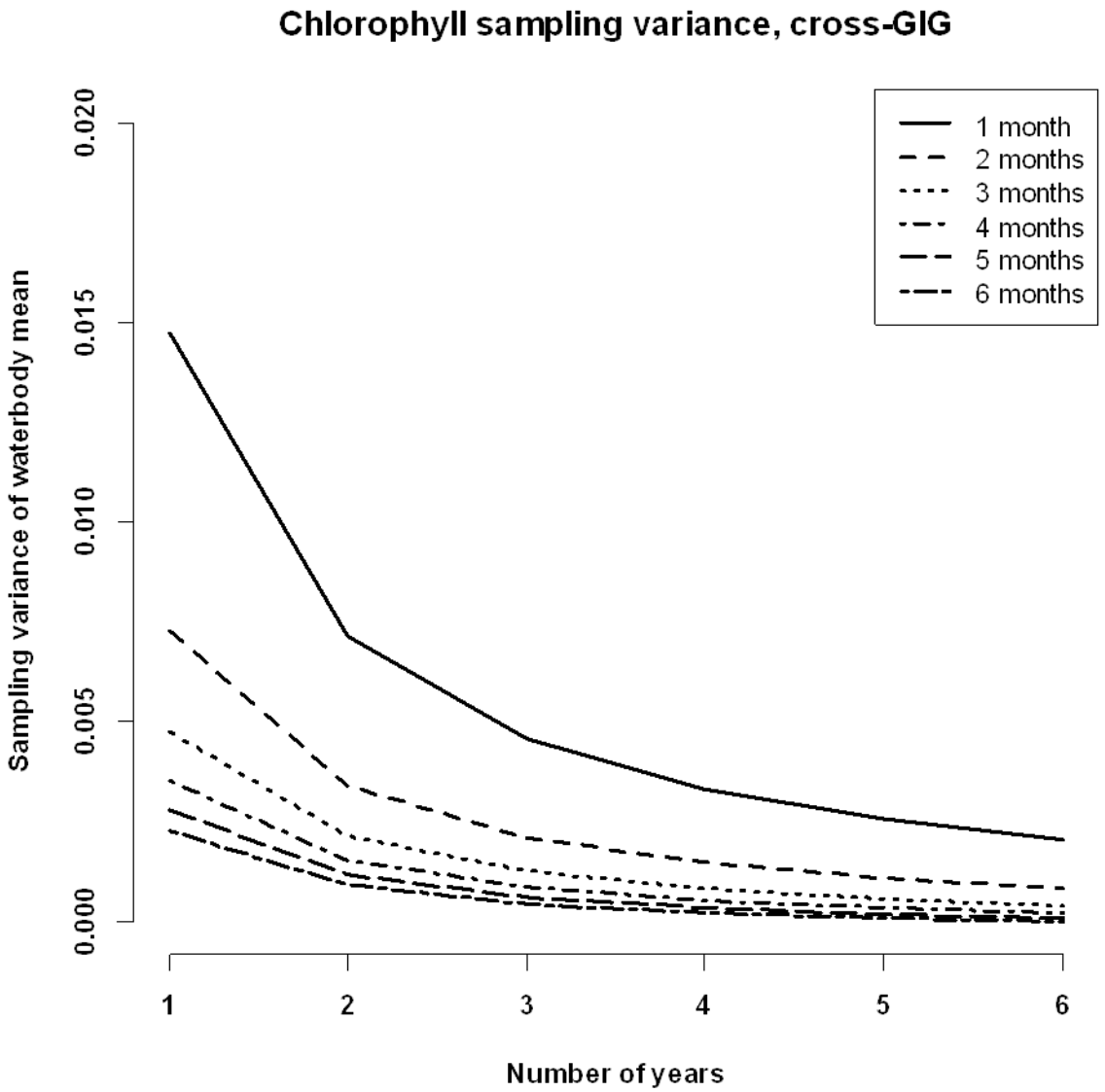

Fig. 1. Changes in monthly and inter-annual scale temporal sampling variance for chlorophyll a, assuming monitoring schemes which differ in the number of years and months-per-year sampled. Analysis based upon the cross-GIG data set.

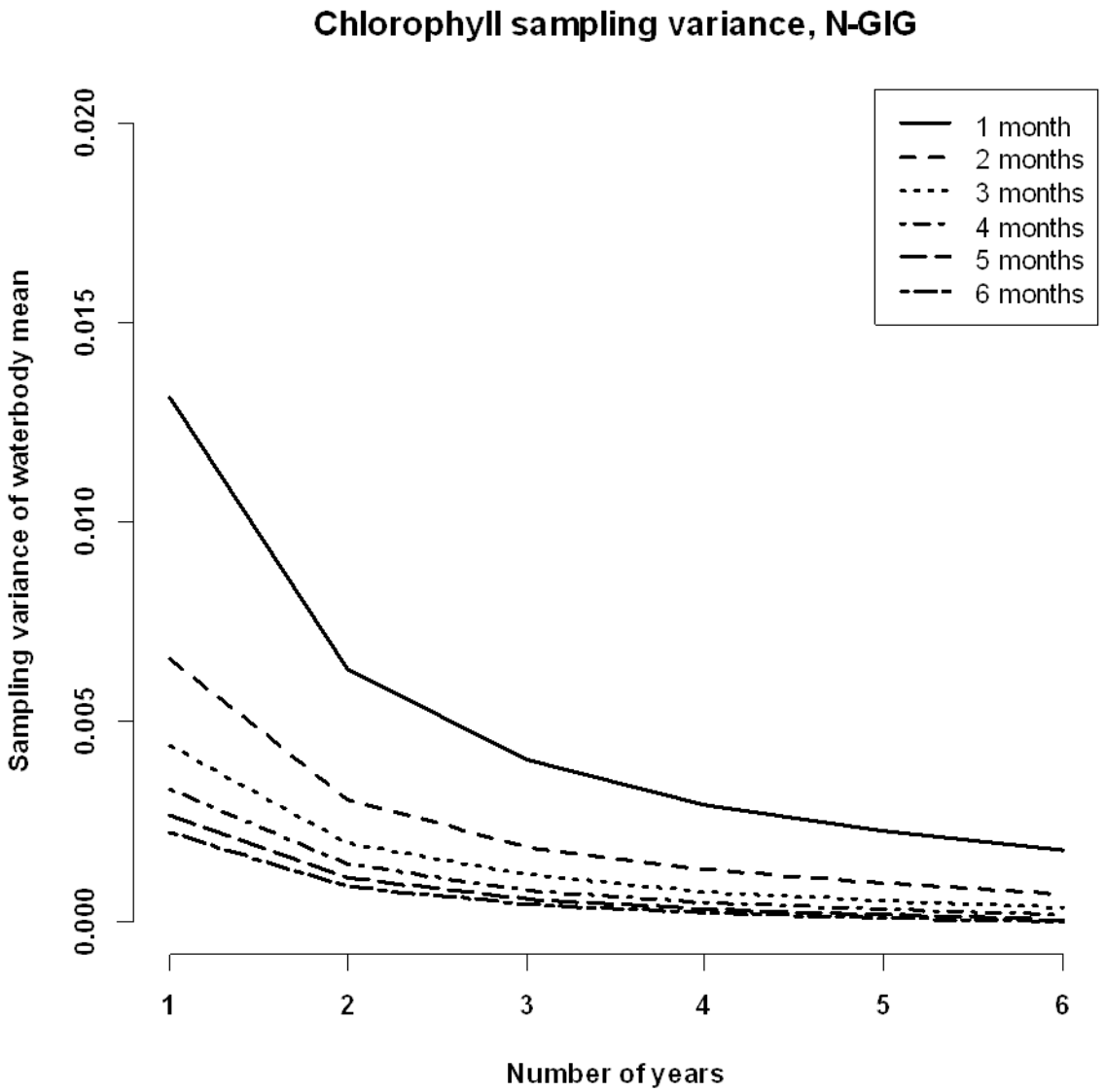

Fig. 2. Changes in monthly and inter-annual scale temporal sampling variance for chlorophyll a, assuming monitoring schemes which differ in the number of years and months-per-year sampled. Analysis based upon the N-GIG data set.

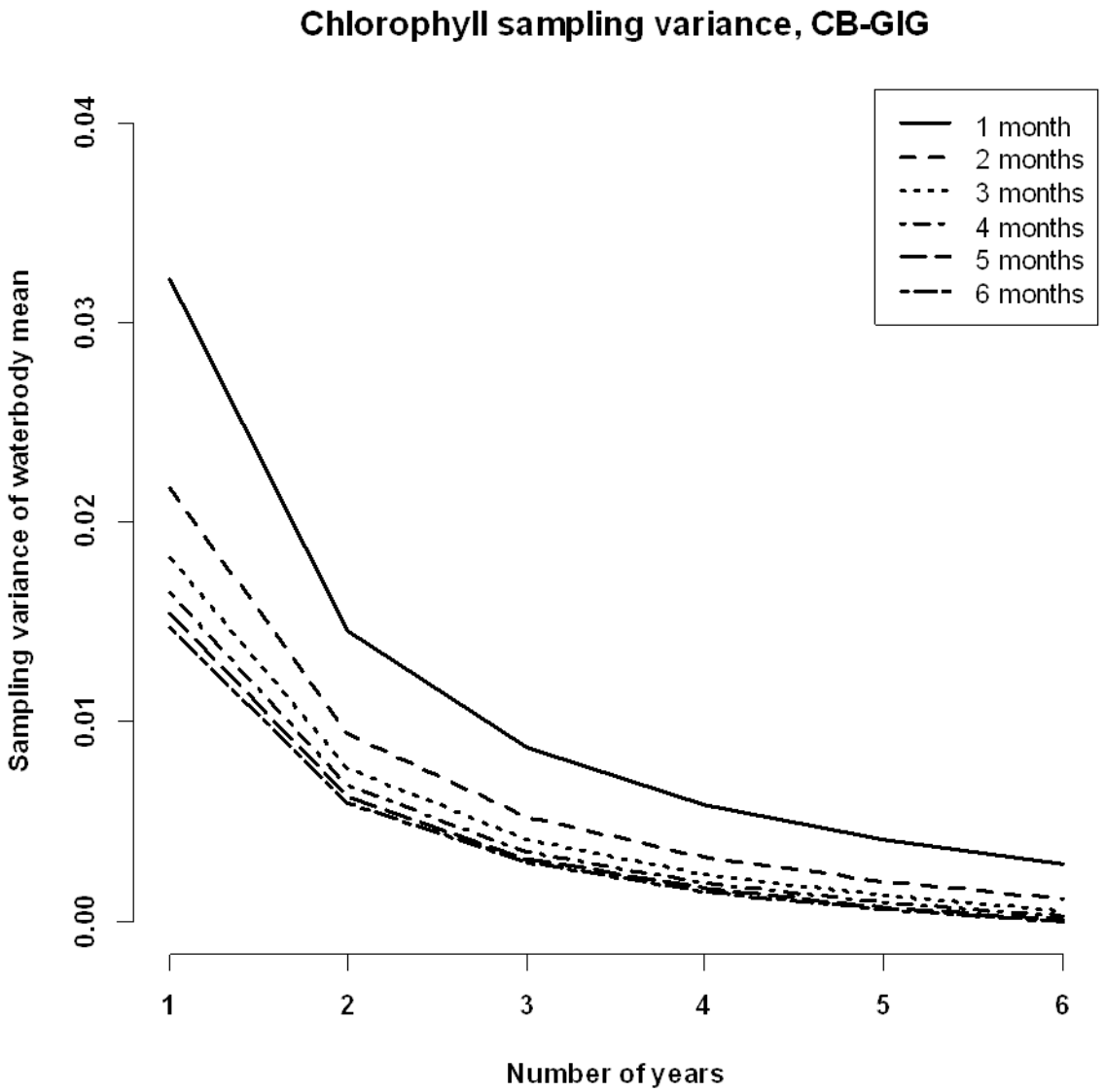

Fig. 3. Changes in monthly and inter-annual scale temporal sampling variance for chlorophyll a, assuming monitoring schemes which differ in the number of years and months-per-year sampled. Analysis based upon the CB-GIG data set. Note difference in scale compared to N-GIG and cross-GIG analyses.

PTI metric

The PTI metric was not transformed prior to analysis. Analyses used data from July-September. Analyses were conducted using the *nlme, MuMIn* and *effects* packages in R (Fox 2003, R Development Core Team 2009, Pinheiro et al. 2010, Barton 2011), assuming Gaussian errors.

- For the all-GIG analysis, and considering instances were all lake attribute data were present, 5186 rows of data were available, from 1253 waterbodies in 13 countries. There were relatively few high altitude data, and so these were combined with medium altitude data. The most optimal fitted models suggested that monthly variation in PTI scores is affected by $\log_{10}$ TP concentration and longitude.
- For the N-GIG analysis, 3900 rows of data were available from 782 waterbodies in 5 countries. The most optimal fitted models suggested that the monthly pattern of variation in PTI scores (in N-GIG) is affected by latitude, longitude, lake type and $\log_{10}$TP concentration.
- For the CB-GIG analysis, 1243 rows of data were available from 450 waterbodies in 8 countries. Within the CB-GIG, alkalinity type and altitude type were redundant as the vast majority of lakes were of high alkalinity and at low altitude. Humic type representation was also highly unbalanced: the majority of lakes had low humic content. These variables were therefore omitted from the analysis. The most optimal fitted models suggested that the monthly pattern of variation in PTI scores (in CB-GIG) is affected by longitude and $\log_{10}$TP concentration.
- For the Med-GIG analysis, 398 rows of data were available from 173 waterbodies in 5 countries. However, this dataset is diminished drastically if only taking cases where all waterbody typology variables are known. Therefore, only interactions among monthly patterns in PTI scores and $\log_{10}$TP concentration were modelled. Very few incidences of sub-monthly scale sampling were found in this subset of the background dataset, such that models attempting to distinguish monthly and within-monthly variability in metric scores failed to converge. Therefore, only models comparing inter-annual and spatial (among country and waterbody) components of variation could be run.
- Analysis at the cross-GIG scale, as well as for N-GIG and CB-GIG data, suggested that the variance in PTI scores among countries and waterbodies was greater than the temporal variance (Table 2). However, the residual variance σ^2_r was consistently higher than either the monthly or inter-annual temporal variance, especially for CB-GIG and Med-GIG.
- The formula for the monthly and inter-annual temporal sampling variance (above) was used following the cross-GIG, N-GIG and CB-GIG analyses, in which it was possible to distinguish monthly and inter-annual variance components (Figs. 4-6). From these analyses, it can be seen that this component of the sampling variance (and associated uncertainty) reduces markedly when increasing the number of months sampled from 1 per year to 2 per year and when sampling in 2-3 years, instead of 1.

All analyses suggest that sampling variance can be reduced dramatically by sampling in 2 months, in each of 3 years. In contrast to the findings for chlorophyll-*a*, there are only modest differences in the level of temporal uncertainty for the PTI metric, when comparing N-GIG and CB-GIG.

Table 2. Components of variation in PTI, expressed as variances.

Variance component	**Cross-GIG**	**N-GIG**	**CB-GIG**	**Med-GIG**
Country, σ^2_c	0.280	0.058	0.070	0.031
Waterbody, σ^2_w	0.181	0.202	0.080	0.143
Total spatial* ($\sigma^2_c + \sigma^2_w$)	**0.462**	**0.260**	**0.150**	**0.174**
Year, σ^2_y	0.014	0.015	0.024	0.015
Month, σ^2_m	0.023	0.024	0.019	-
Residual, σ^2_r	0.043	0.028	0.076	0.096
Total temporal ($\sigma^2_y + \sigma^2_m$)	**0.037**	**0.039**	**0.042**	**0.015**

*spatial variance components were derived from a mixed-effects model with an intercept only (i.e. a null model).

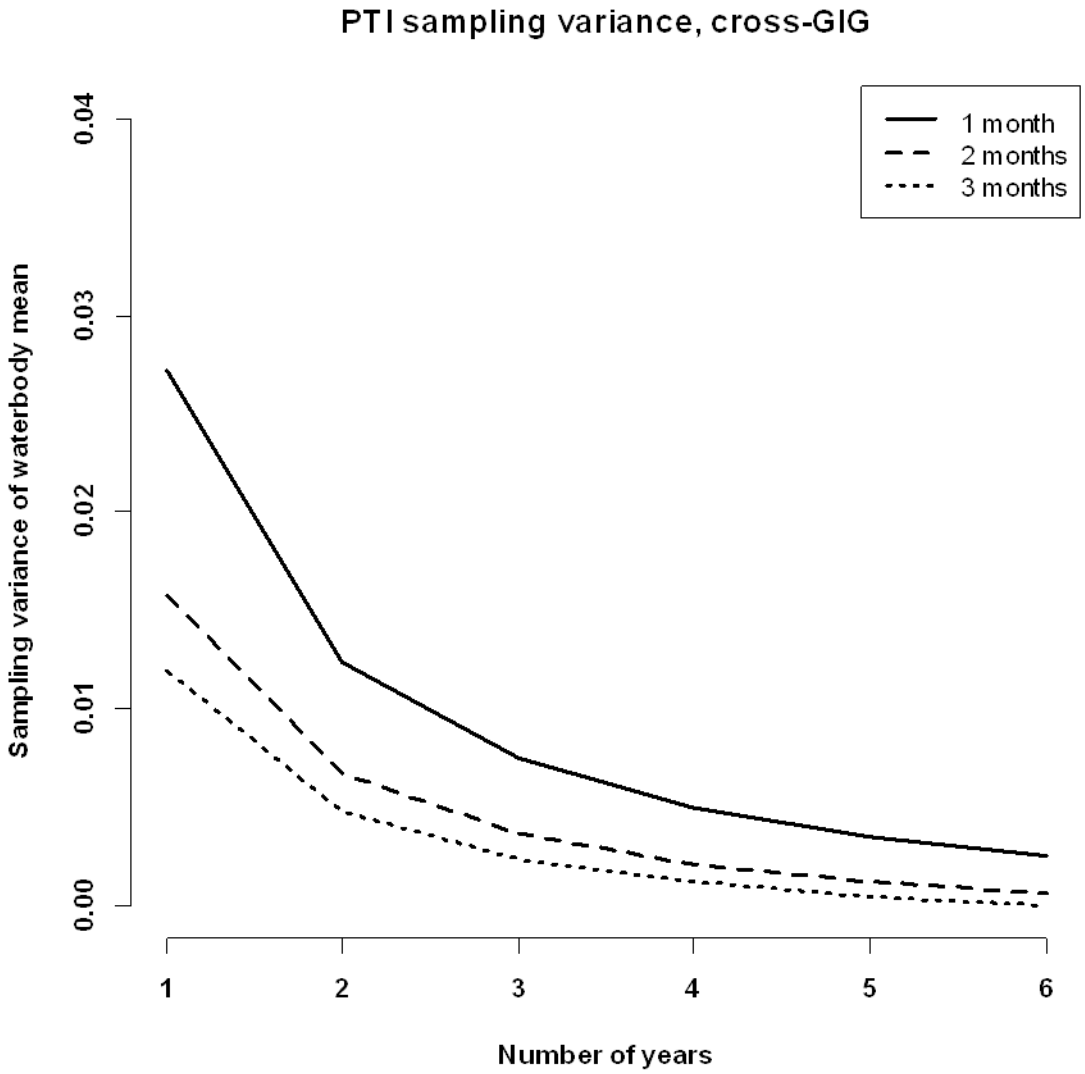

Fig. 4. Changes in the monthly and inter-annual scale temporal sampling variance for the PTI metric, assuming monitoring schemes which differ in the number of years and months-per-year sampled. Analysis based upon the cross-GIG data set.

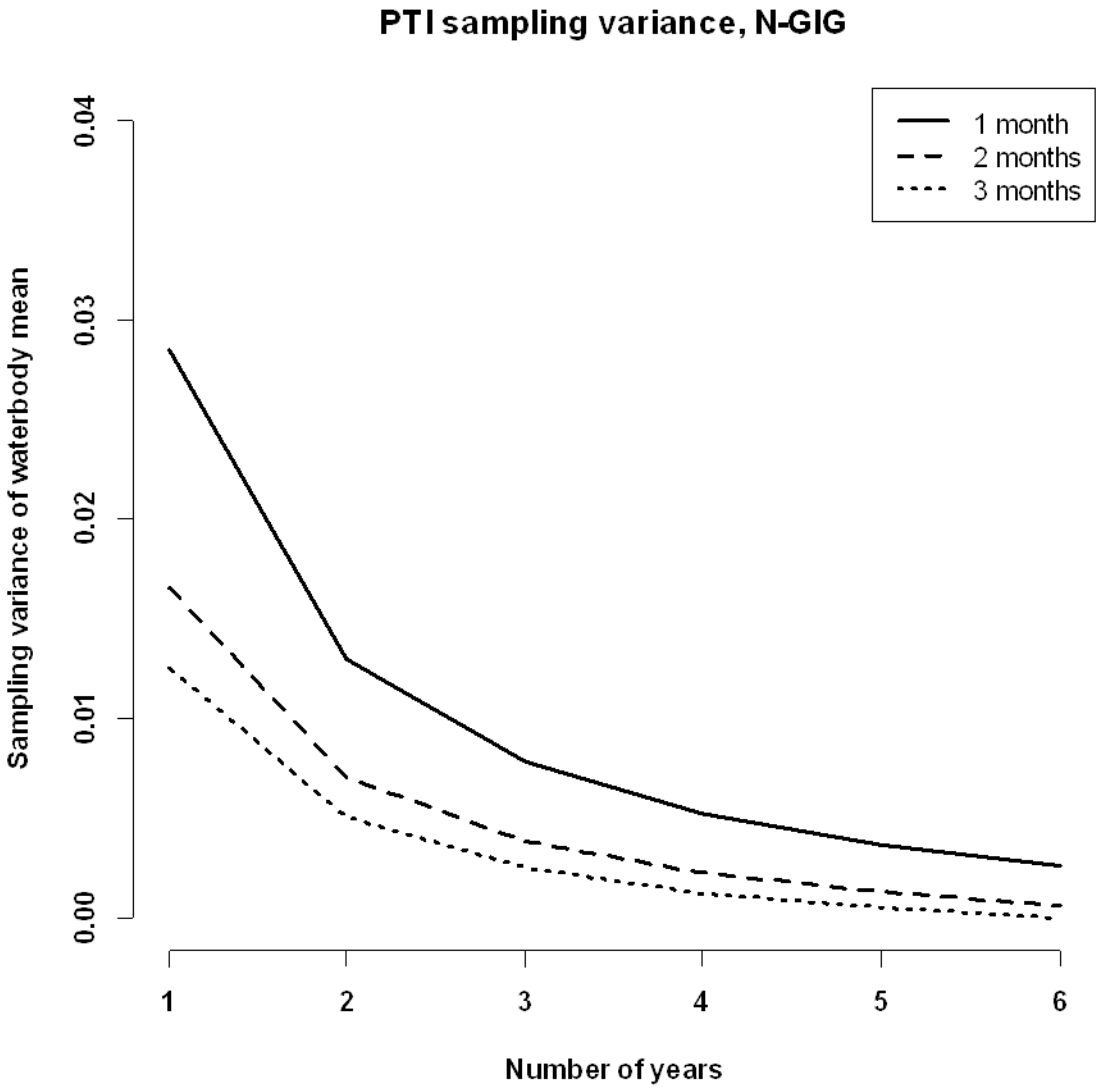

Fig. 5. Changes in the monthly and inter-annual scale temporal sampling variance for the PTI metric, assuming monitoring schemes which differ in the number of years and months-per-year sampled. Analysis based upon the N-GIG data set.

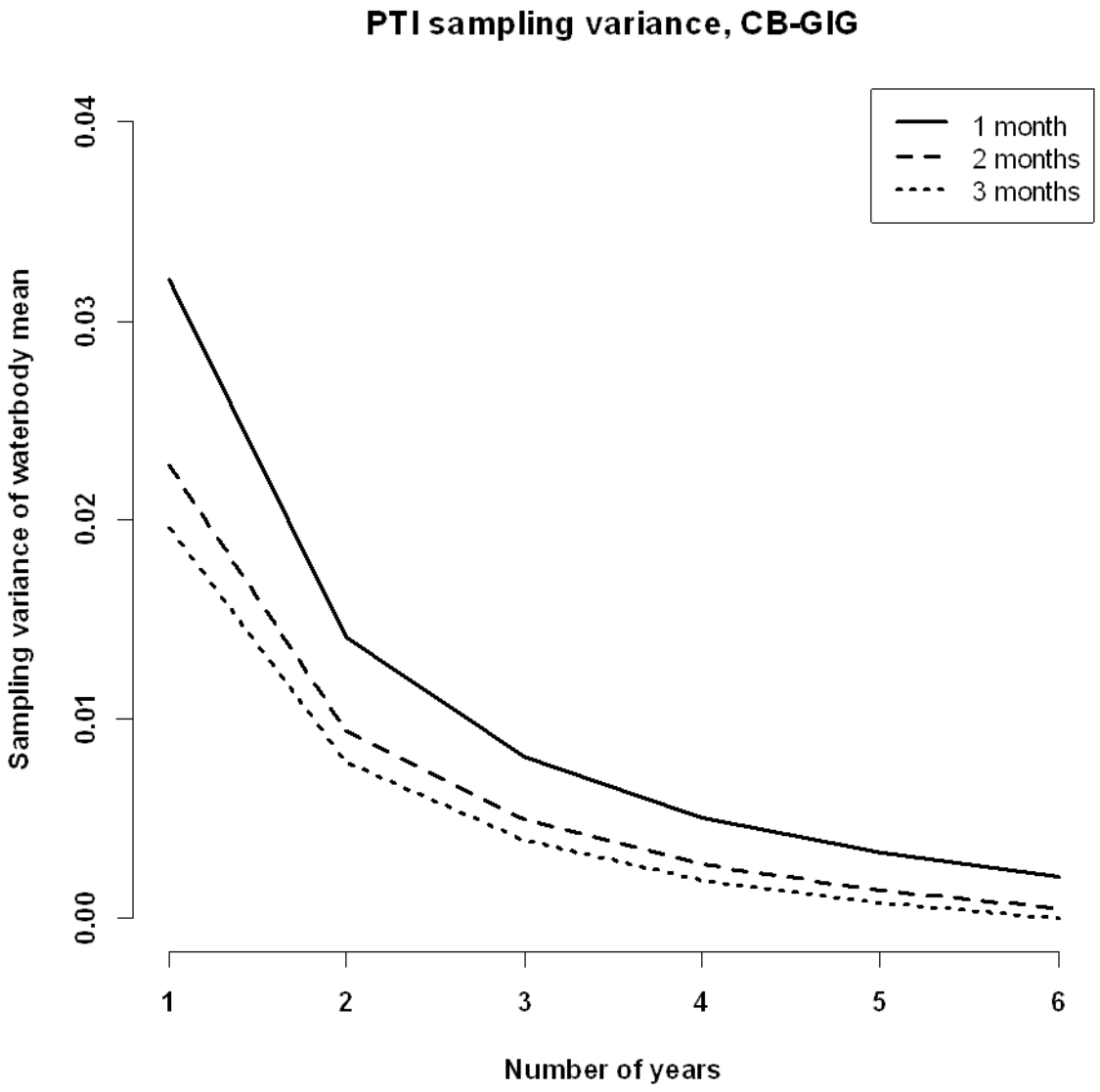

Fig. 6. Changes in the monthly and inter-annual scale temporal sampling variance for the PTI metric, assuming monitoring schemes which differ in the number of years and months-per-year sampled. Analysis based upon the CB-GIG data set.

Total cyanobacterial biovolume (TCB)

The TCB metric was $\log_{10}$ transformed prior to analysis. Model selection and fitting was performed using *MCMCglmm* package (Hadfield 2010) in R (R Development Core Team 2009) and comparison of DIC values. Convergence of the chains was checked using the Gelman-Rubin-Brooks plots and diagnostics from the *coda* package (Plummer et al. 2006). Analyses used data from July-September. An exponential error structure was incorporated into the model for all analyses. Therefore, variance estimates are based on the metric on the exponential scale.

- For the all-GIG analysis, and considering instances where all lake attribute data were present, 5186 rows of data were available, from 1253 waterbodies in 13 countries. The most optimal fitted models suggested that the monthly pattern of variation in the TCB metric is affected by $\log_{10}$TP concentration, at the cross-GIG scale.
- For the N-GIG analysis, 3900 rows of data were available from 782 waterbodies in 5 countries. The most optimal fitted models suggested that the monthly pattern of variation in the TCB metric (in N-GIG) is not affected by any of the variables examined.
- For the CB-GIG analysis, 1243 rows of data were available from 450 waterbodies in 8 countries. Within the CB-GIG, alkalinity type and altitude type were redundant as the vast majority of lakes were of high alkalinity and at low altitude. Humic type representation was also highly unbalanced: the majority of lakes had low humic content. These variables were therefore omitted from the analysis. The most optimal fitted models suggested that the monthly pattern of variation in the TCB metric (in CB-GIG) is affected by $\log_{10}$TP concentration.
- For the Mediterranean GIG analysis 398 rows of data were available from 173 waterbodies in 5 countries. However, this dataset is diminished drastically if only taking cases where all waterbody typology variables are known. Therefore, only interactions between monthly patterns in the TCB metric and $\log_{10}$TP concentration were modelled. Very few incidences of sub-monthly scale sampling were found in this subset of the background dataset, such that models attempting to distinguish monthly and sub-monthly variability in metric scores could not be run. Therefore, only models comparing inter-annual and spatial (among country and waterbody) components of variation were run. There was no significant monthly pattern in the variation in the metric with the level of $\log_{10}$TP. Therefore, the yearly variance was estimated from a model fitted with only $\log_{10}$TP as a fixed effect. For the Med-GIG analyses, the spatial variation is the main source of variation in the TCB metric.
- Analysis at the cross-GIG scale, as well as for N-GIG and CB-GIG data, suggested that the variance in the TCB metric among countries and waterbodies was greater than the temporal (monthly, inter-annual) variance (Table 3). For Med-GIG, inter-annual variance in the TCB metric was less than among country and waterbody variance.

However, the residual variance σ^2_r was frequently much higher than either the monthly or inter-annual metric variance components.

- The formula for monthly and inter-annual scale temporal sampling variance (above) was used following the cross-GIG, N-GIG and CB-GIG analyses (Figures 7-9), in which it was possible to distinguish monthly and inter-annual variance components. From these analyses for the cross-GIG and N-GIG data, it can be seen that the sampling variance (and associated uncertainty) reduces when increasing the number of months sampled per year and when sampling in 3-4 years. For the CB-GIG analysis, the sampling variance does not reduce markedly when increasing the number of months sampled, but it does when increasing the number of years sampled from 1 year to 2-4 years.

Table 3. Components of variation in $\log_{10}$(total cyanobacterial biovolume +1), expressed as variances from best fit models with an exponential error structure.

Variance component	**Cross-GIG**	**N-GIG**	**CB-GIG**	**Med-GIG**
Country, σ^2_c	13245	20781	0.966	49095
Waterbody, σ^2_w	36264	54332	2.243	9090
Total spatial* ($\sigma^2_c + \sigma^2_w$)	**49509**	**75113**	**3.209**	**58185**
Year, σ^2_y	7637	6907	0.650	28348
Month, σ^2_m	864	659	0.014	-
Residual, σ^2_r	35854	41956	0.015	43880
Total temporal ($\sigma^2_y + \sigma^2_m$)	**8501**	**7566**	**0.664**	**28348**

*spatial variance components were derived from a mixed-effects model with no explanatory variables (i.e. a null model).

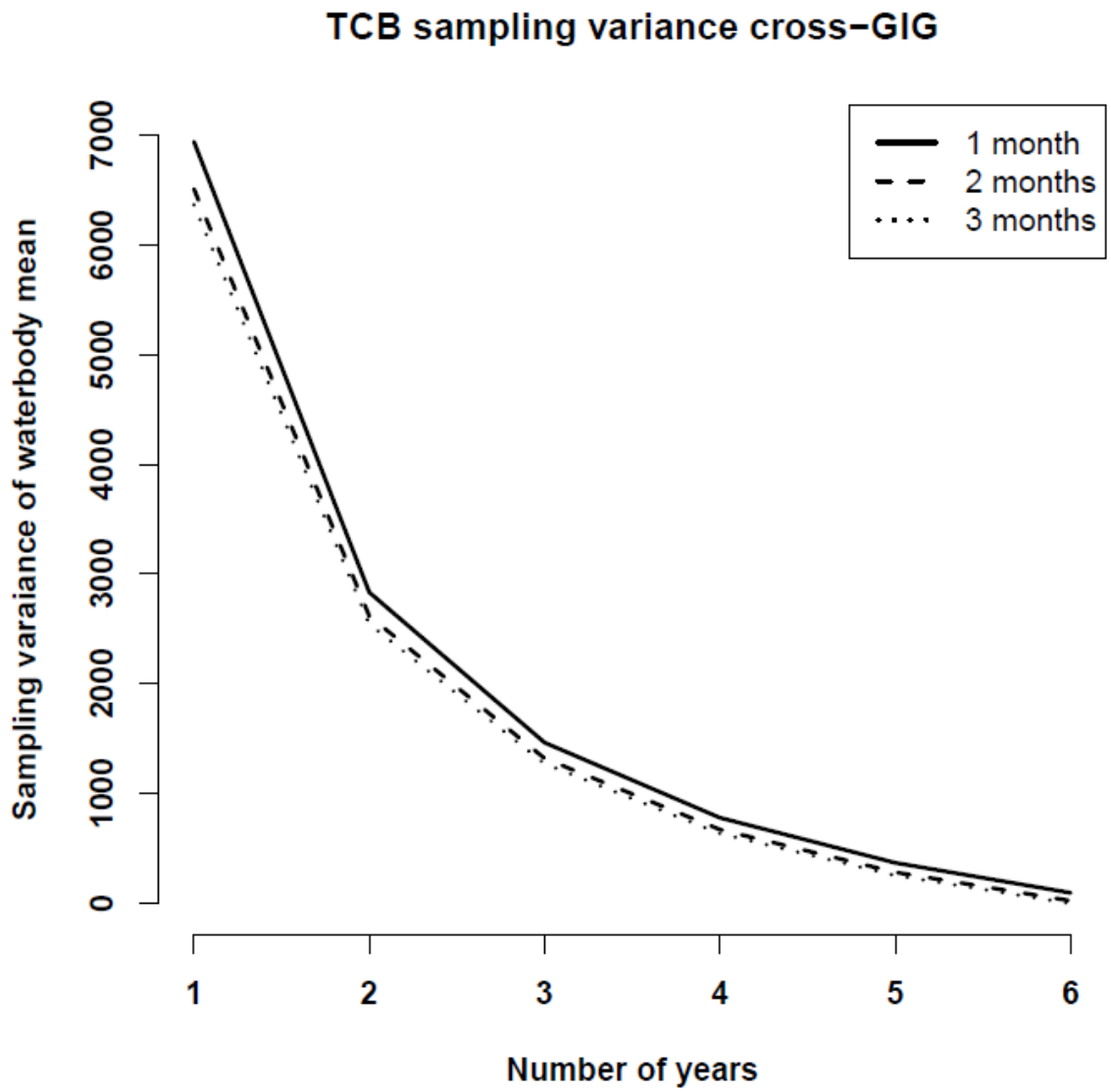

Fig. 7. Changes in the monthly and inter-annual scale temporal sampling variance for the TCB metric, assuming monitoring schemes which differ in the number of years and months-per-year sampled. Analysis based upon the cross-GIG data set.

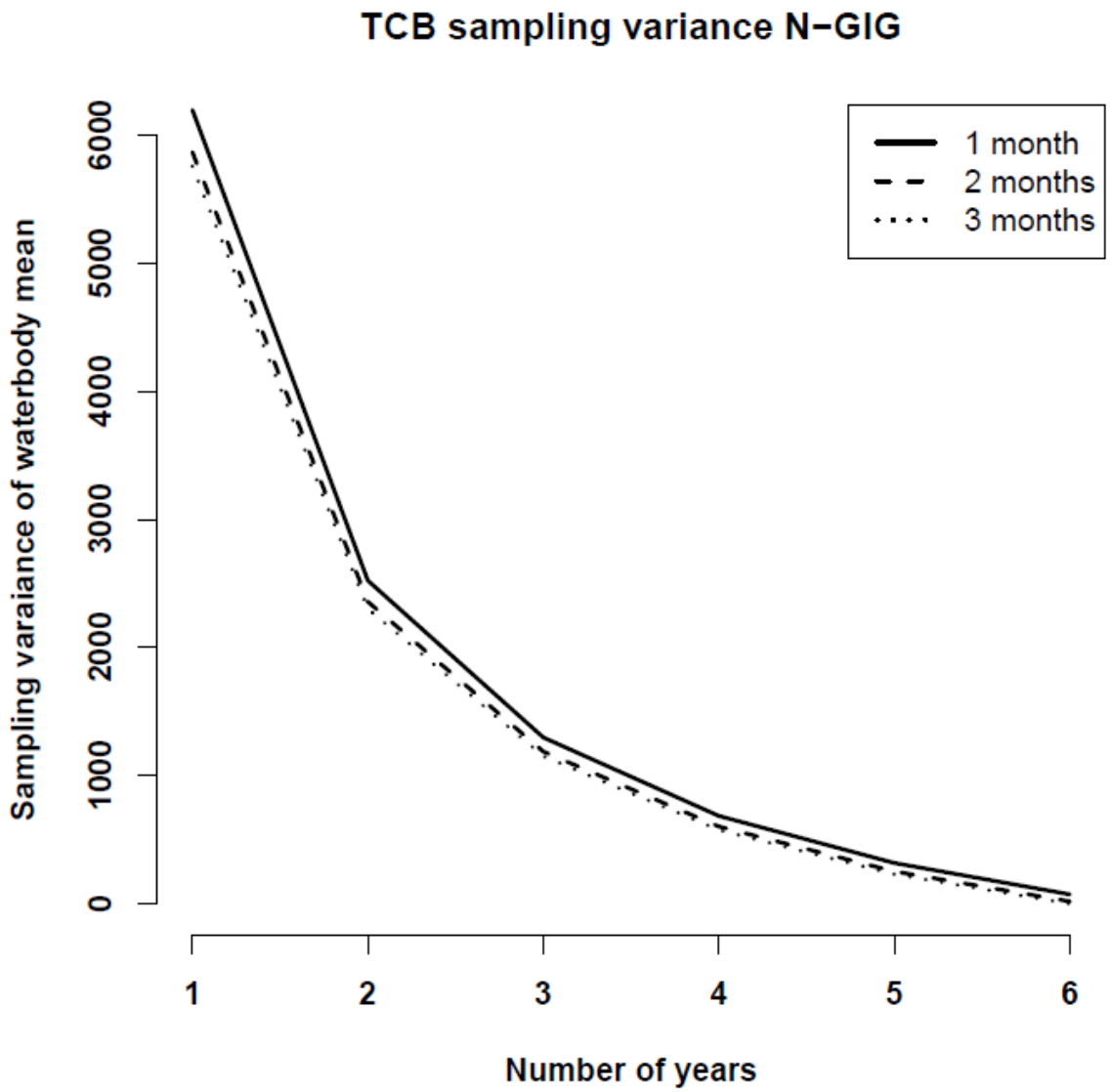

Fig. 8. Changes in the monthly and inter-annual scale temporal sampling variance for the TCB metric, assuming monitoring schemes which differ in the number of years and months-per-year sampled. Analysis based upon the N-GIG dataset.

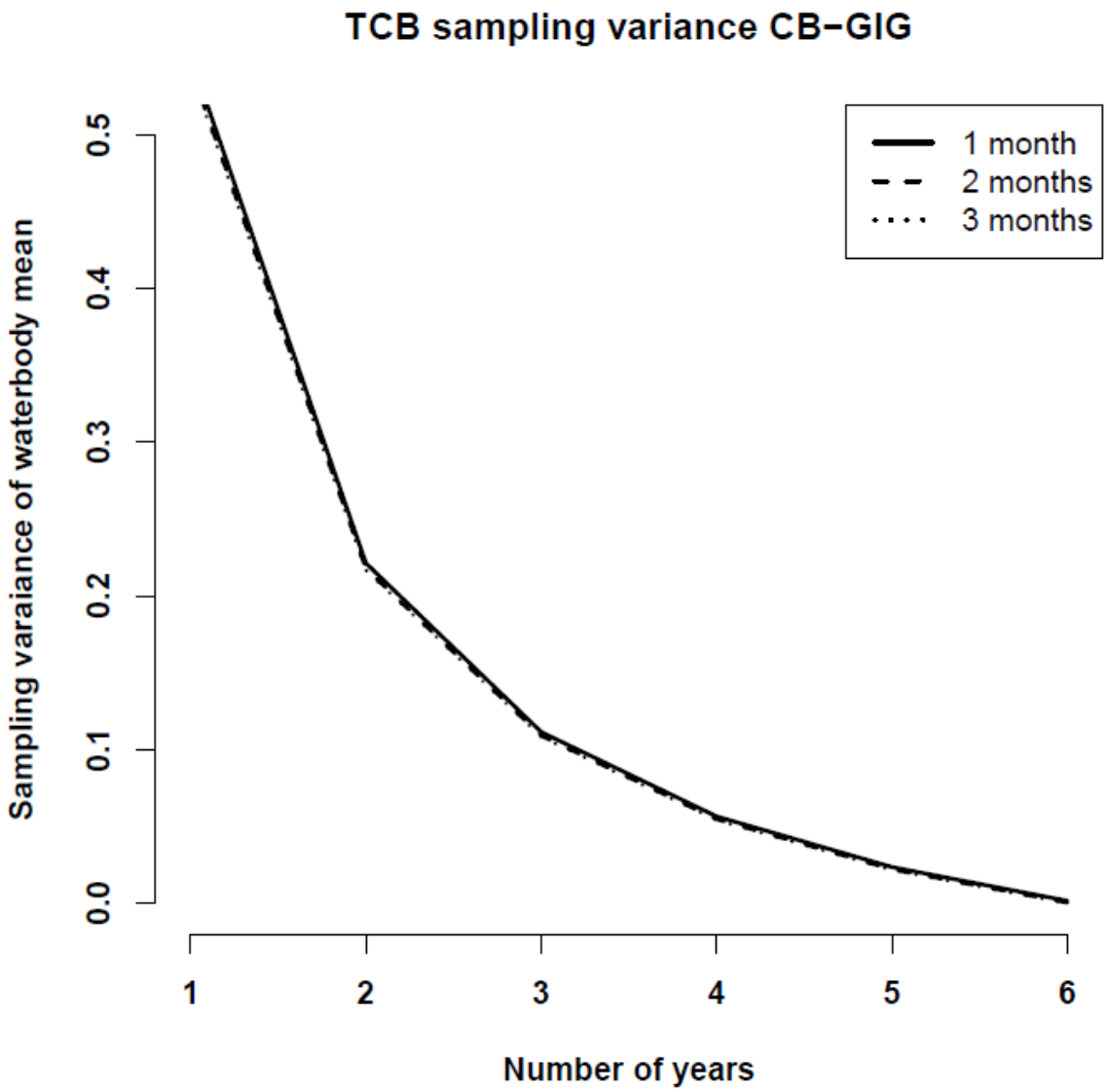

Fig. 9. Changes in the monthly and inter-annual scale temporal sampling variance for the TCB metric, assuming monitoring schemes which differ in the number of years and months-per-year sampled. Analysis based upon the CB-GIG data set.

Key messages

- For $\log_{10}$ Chl-*a* concentration, PTI and $\log_{10}$ total cyanobacterial biovolume, inter-annual and monthly temporal variation was less than that found among waterbodies distributed along a wide pressure gradient. This would suggest that monthly and inter-annual scale temporal variation in these metrics is not of a great enough magnitude to occlude differences between systems that are experiencing different lake-level pressures.
- However, residual metric variance (σ^2_r) was frequently high compared to monthly and inter-annual temporal variation. This was especially pronounced for the total cyanobacterial biovolume metric. The magnitude of the estimated residual variance components suggests the presence of additional, important, sources of metric variability. While short-term (within-month) temporal variation in the phytoplankton assemblage will contribute to this variability, σ^2_r will also contain within it other sources of variation that are not directly linked to short-term plankton dynamics e.g. differences in sampling/sample processing procedures and analyst identity (Thackeray et al. 2011). Future analyses are needed to explicitly determine the independent components of σ^2_r in order to quantify short term metric variation, independently of other uncontrolled sources of variation, and within the context of changes at the monthly and inter-annual scales.
- Herein, we have focussed our investigation on how the longer-term aspects of temporal uncertainty (monthly, inter-annual scale) can be affected by monitoring programme design. Estimates of monthly and inter-annual scale temporal sampling variance (i.e. the variability in waterbody mean metric scores that would arise from sampling different combinations of years, and months within each year) show that changes in sampling strategy can reduce this component of temporal uncertainty in metric scores markedly. For the PTI metric in N-GIG and CB-GIG, and $\log_{10}$ Chl-*a* concentration in N-GIG, sampling in 2 months in each of 3 years would achieve a marked reduction in temporal metric uncertainty. For $\log_{10}$ Chl-*a* concentration in CB-GIG, more temporal replication would be needed to achieve this same level of reduction in uncertainty. For the total cyanobacterial metric, a greater number of years may need to be sampled to reduce the overall monthly and inter-annual scale temporal sampling variance. In N-GIG, sampling in 2 months in each of 4 years would reduce the inter-annual and monthly component of metric uncertainty considerably, but for CB-GIG an increase in the number of sampling months would not have a major effect on sampling uncertainty.
- There is no single best solution in terms of sampling frequency, since temporal sampling uncertainty will always diminish with increasing temporal replication. The key issue is the need to reach an optimal trade-off between the need for monitoring precision, and the costs of monitoring itself. However, please note that the notion of reaching an optimally cost-effective frequency of sampling (expressed simply in terms of *numbers* of months and *numbers* of years sampled) implicitly assumes that months and years are fully substitutable e.g. all months within the predetermined seasonal

window are ecologically equivalent. This assumption may not be met in real communities.

- Attempts to make robust estimates of temporal and spatial components of variation in phytoplankton metrics are dependent upon having detailed and comprehensive monitoring data. It is necessary for sample data to be available for different months across a number of years, but also for multiple dates within months (at least in some cases). Furthermore, lake attribute/classification variables are essential if we are to fit biologically meaningful models that can capture gradients in the seasonality of phytoplankton communities.
- Results from the $\log_{10}$ Chl-*a* and total cyanobacterial biovolume analyses suggested that temporal variation did vary by GIG, and that different levels of temporal sample replication would be needed to achieve the same level of precision in waterbody mean metric values in different GIGs. Therefore, decisions on optimal sampling frequency may also differ by GIG.
- Our approach suggested that among-lake differences in the seasonal, within-year, patterns in phytoplankton metrics could be modelled effectively with the available explanatory variables. We will explore this further in a temporal uncertainty paper.

References

Barton, K. 2011. MuMIn: Multi-model inference. R package version 1.0.0. <http://CRAN.R-project.org/package=MuMIn>.

Fox, J. 2003. Effect Displays in R for Generalised Linear Models. Journal of Statistical Software **8**:1-27.

Hadfield, J. D. 2010. MCMC Methods for Multi-Response Generalized Linear Mixed Models: The MCMCglmm R Package. Journal of Statistical Software **33**:1-22.

Pinheiro, J., D. Bates, S. DebRoy, D. Sarkar, and R Development Core Team. 2010. nlme: Linear and nonlinear mixed effects models. R package version 3.1-97.

Plummer, M., N. Best, K. Cowles, and K. Vines. 2006. CODA: Convergence Diagnosis and Output Analysis for MCMC. R News **6**:7-11.

R Development Core Team. 2009. R: A language and environment for statistical computing. R Foundation for Statistical Computing, Vienna, Austria.

Thackeray S.J., Nõges P., Dunbar M., Dudley B., Skjelbred B., Morabito G., Carvalho L., Phillips G. & Mischke U. (2011): Deliverable D3.1-3: Uncertainty in Lake Phytoplankton Metrics. 42p. http://www.wiser.eu/results/deliverables/